

NUMERICAL CALCULATIONS OF THE RADIATION EMITTED FROM THE FLASH INFRARED UNDULATOR

O. Grimm*, J. Rossbach, University of Hamburg
V. Kocharyan, DESY, Hamburg, Germany

Abstract

The VUV and soft X-ray free-electron laser FLASH at DESY, Hamburg, has been complemented with an infrared undulator working in the wavelength range of 1 to 200 μm , providing pulses naturally synchronized with the FEL radiation. The results from the magnetic measurements prior to installation are used here as input for calculations of the expected radiation spectrum. Especially the behavior at small excitation currents is important for beam diagnostics using coherent radiation.

INTRODUCTION

Complementing the FLASH facility at DESY, Hamburg, with an undulator working in the mid- and far-infrared regime was first proposed in [1]. There is a strong interest in using such an undulator delivering up to 10 MW peak power in the THz-regime as a radiation source, allowing pump-probe experiments with high temporal resolution. Another equally important application lies within longitudinal bunch shape diagnostics [2, 3]. More details on the undulator have been reported in [4, 5].

The device has been build and installed in the FLASH accelerator, with first beam passing through expected in September 2007. In [6] results of the magnetic measurements that were performed prior to installation are reported. These are used for detailed numerical calculations of the radiation characteristics, some of which are reported in this paper. Such calculations are necessary input to optics codes to quantitatively analyze the transmission characteristics of the infrared beam line.

NUMERICAL CODES

Several numerical codes have been used to perform calculations of the radiation characteristics. Comparisons between the results from different codes are mandatory to get confidence about their validity.

Many calculations are performed with a custom-made code written in Matlab called SynchroSim. The code implements a full time-domain calculation based on using the general Liénard-Wiechert fields from an accelerated charge [7] and a subsequent Fourier transformation to get the spectrum. There are no approximations involved, however the calculation speed is low. Alternatively, a direct calculation in frequency-domain can be done using the paraxial

approximation of synchrotron radiation emission [8], giving much higher speed.

The Synchrotron Radiation Workshop (SRW) code has also been used extensively [9]. Some cross-checks were performed with the SPECTRA code [10].

Perfect agreement was found for on-axis spectra calculated with SRW, SPECTRA and SynchroSim. The transverse intensity distribution at 61 μm wavelength and 1 GeV energy is compared between SRW and SynchroSim in Fig. 1. Also here very good agreement is found.

The horizontally asymmetric distribution and interference fringes result mainly from the undulator end poles. Some contribution results also from the inclusion of the dipole magnet that is installed downstream of the undulator. It has a field of about 0.45 T at 500 MeV and is used to dump the electron beam. It should be noted that further along the infrared beam line the relative contribution of the dipole will reduce, as the optics is optimized for the radiation contribution from the undulator.

Further comparisons confirmed the good agreement between different codes, thus calculations in the following were performed with the most convenient program.

SPECTRUM CALCULATIONS

The spectrum calculated for 200 A excitation current of the undulator at 511 MeV electron energy is shown in Fig. 2. On-axis a typical resonance spectrum is obtained containing only odd harmonics. When integrating over a transverse area of $60 \times 60 \text{ mm}^2$ (corresponding to the beam line acceptance at that position), the spectrum acquires a clear baseline. This is an indication of the fact that only a small fraction of the total energy emitted by an electron ends up within the harmonics, see the estimation in the last section.

This effect becomes more pronounced at smaller excitation currents, as Fig. 3 shows for 30 A. This is due to the reduced opening angle of the harmonics at smaller K value, and thus larger contribution of non-resonant radiation when the acceptance aperture is fixed.

TRANSVERSE INTENSITY CALCULATIONS

The transverse distributions of the total radiation intensity (summed over both polarizations) with the undulator current set to the maximum value of 435 A is shown in Fig. 4 for the first and third harmonic (192 μm and 64 μm at 511 MeV, respectively). The 60 mm diameter aperture of

* Corresponding author. E-Mail: oliver.grimm@desy.de

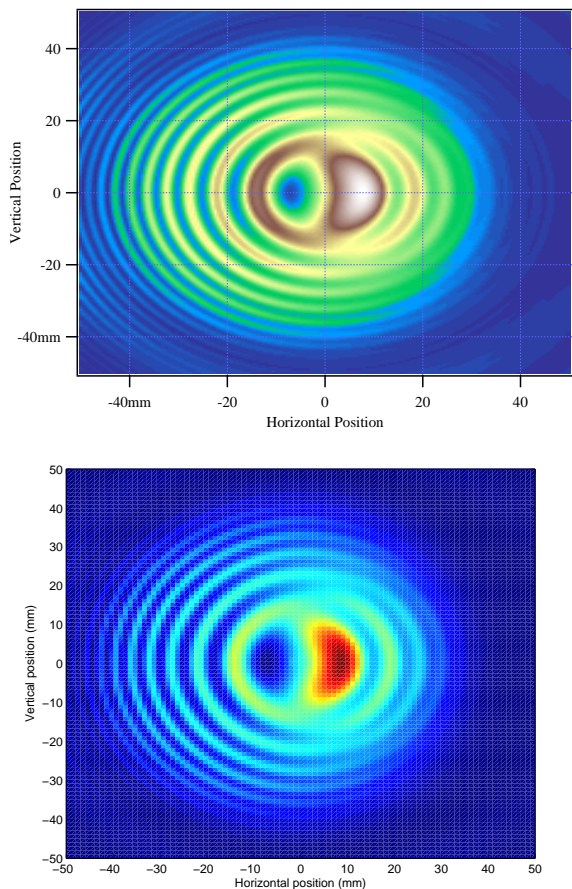


Figure 1: Transverse intensity distribution 9 m behind the undulator centre at $61 \mu\text{m}$ wavelength and 1 GeV energy. Top: SRW, bottom: SynchroSim.

the beam transport line at that position clips the first harmonic. This reduction of the harmonic amplitude has to be taken into account for beam diagnostics, as the coherent amplification due to the form factor of the longitudinal charge distribution is imprinted on the relative height of the harmonics.

These plots were calculated at a single wavelength exactly on resonance. Any measurement will be integrated over a certain range. Fig. 5 shows the intensity distribution of the first harmonic at 30 A excitation current both for a wavelength on resonance and when integrated over the 10% harmonic bandwidth.

Fig. 6 finally shows the transverse intensity distribution for both polarizations at 30 A when integrated over the full bandwidth of Fig. 3.

TOTAL EMITTED ENERGY

At high K parameter, the spectrum is wiggler-like, consisting of a large number of harmonics. This can be easily understood qualitatively by approximating the undulator for that case as a series of 18 bending magnets of opposite polarity (as the undulator has 9 full periods), sep-

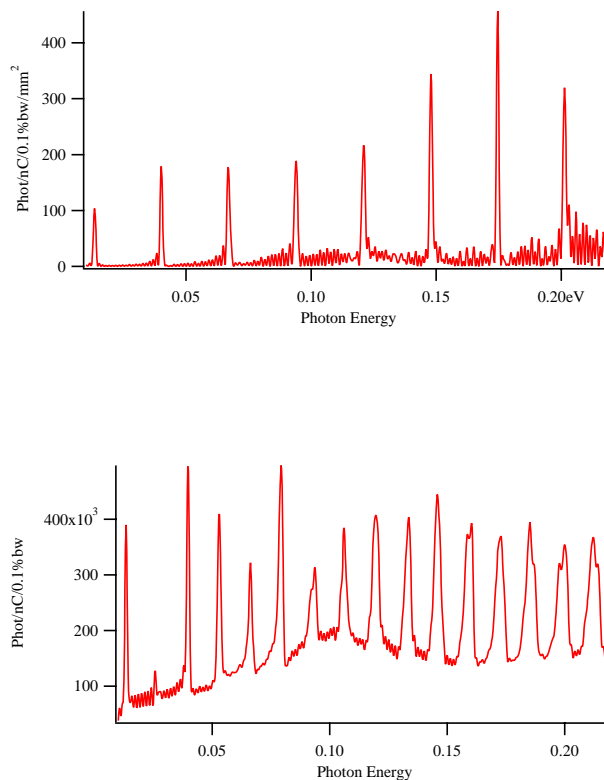


Figure 2: Spectrum at 200 A excitation current and an energy of 511 MeV. On-axis spectrum (top) and integration over a transverse area of $60 \times 60 \text{ mm}^2$. The first harmonic is at $92 \mu\text{m}$.

arated by half a fundamental wavelength. The spectrum emitted by one bend (approximated as that from circular motion synchrotron radiation) will then be modified into a line spectrum, as Fig. 7 shows.

This approach allows to deduce a scaling of the pulse energy within a given harmonic n . From [11], the bandwidth for an undulator with N periods and fundamental frequency ν_0 is

$$\Delta\nu/\nu \approx 1/(Nn), \quad \nu = n\nu_0,$$

and the solid angle subtended by the central cone for the relativistic gamma factor γ

$$\Omega \approx \pi \frac{1 + K^2/2}{2\gamma^2 Nn} \stackrel{K \gg 1}{\approx} \frac{\pi K^2}{4\gamma^2 Nn}.$$

The envelope \mathcal{E} of the harmonics amplitude in Fig. 7 follows from the low-frequency expression of the synchrotron radiation intensity on axis [7]. It scales for a given magnetic field as $\nu^{2/3}$. The scaling of the energy E within one harmonic can thus be estimated as

$$E \sim \mathcal{E} \cdot \Delta\nu \cdot \Omega \sim n^{-1/3}.$$

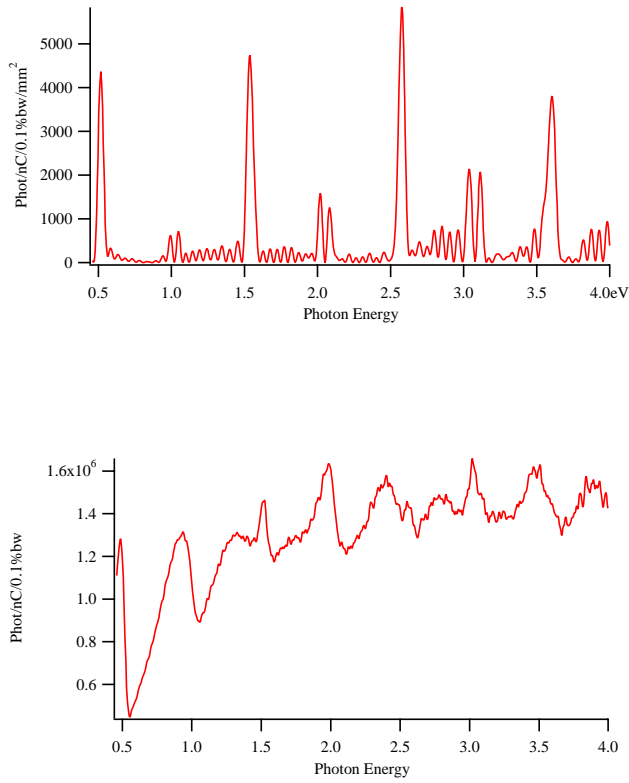


Figure 3: As Fig. 2, but for 30 A excitation current. The first harmonic is at 2.8 μm .

This scaling holds for n much smaller than the harmonic corresponding to the critical frequency: $n \ll 3K^3/8$.

The total energy W_h in all harmonics can be roughly estimated as summing them up to this critical harmonic. Using the expression for the first harmonic energy from [11], this results in

$$W_h \approx \frac{4\pi e^2 \gamma^2}{\epsilon_0 \lambda_u K^2} (J_0(1/2) - J_1(1/2))^2 \cdot \sum_{n=1}^{3K^3/8} n^{-1/3},$$

where λ_u is the undulator period. The total energy W_r radiated by a single electron when passing through an undulator with sinusoidal field can be obtained by integration of the instantaneous power, giving

$$W_r \approx \frac{\pi e^2 \gamma^2 K^2 N}{3\epsilon_0 \lambda_u}.$$

The ratio becomes, by approximately evaluating the Bessel function expression,

$$\frac{W_r}{W_h} \approx \frac{K^4 N}{6 \sum_{n=1}^{3K^3/8} n^{-1/3}}.$$

For $K = 42$, corresponding to a first harmonic at 192 μm for 511 MeV, and $N = 9$ this results in $W_r/W_h \approx 3400$.

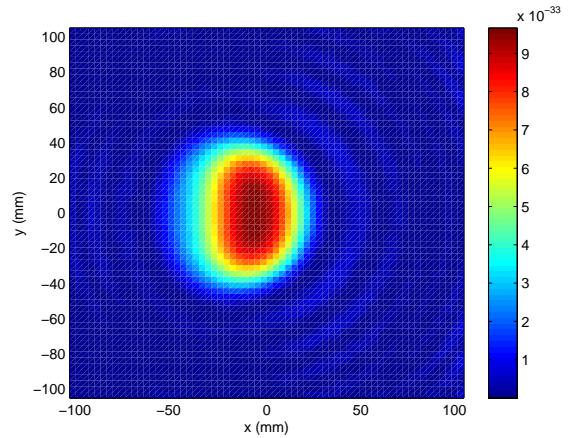
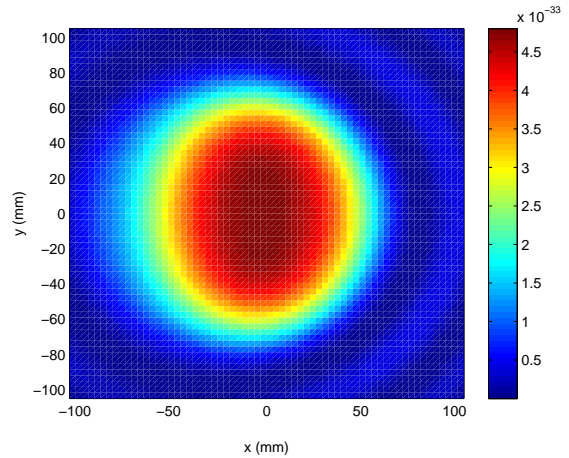


Figure 4: Transverse intensity distribution 10 m behind the undulator centre, at 192 μm (1st harmonic, top) and 64 μm (3rd harmonic, bottom) wavelength. The colour intensity scale is in $\text{J}/(\text{m}^2\text{Hz})$.

Only a very small fraction of the energy lost by an electron actually ends up in one of the harmonics.

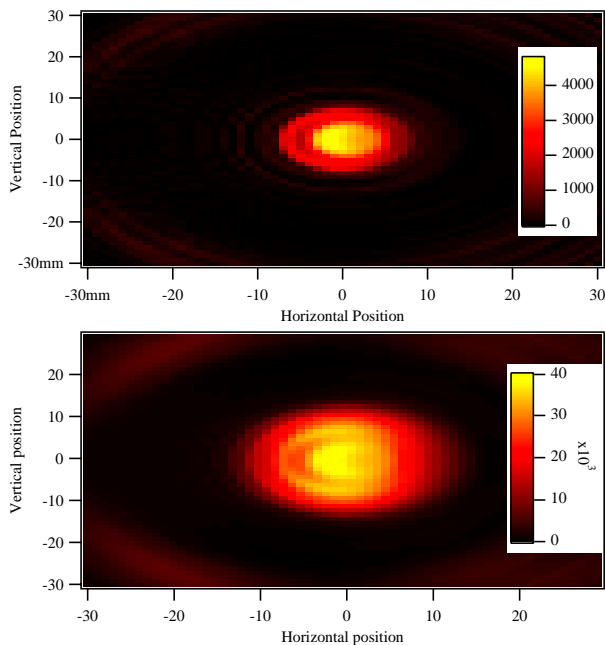


Figure 5: Transverse intensity distribution 10m behind the undulator centre, on resonance of the first harmonic (2.8 μm , top) and integrated over its 10% bandwidth (bottom). Units of the colour scale are photons/(nC mm² 0.1% BW) (top) and photons/(nC mm²) (bottom).

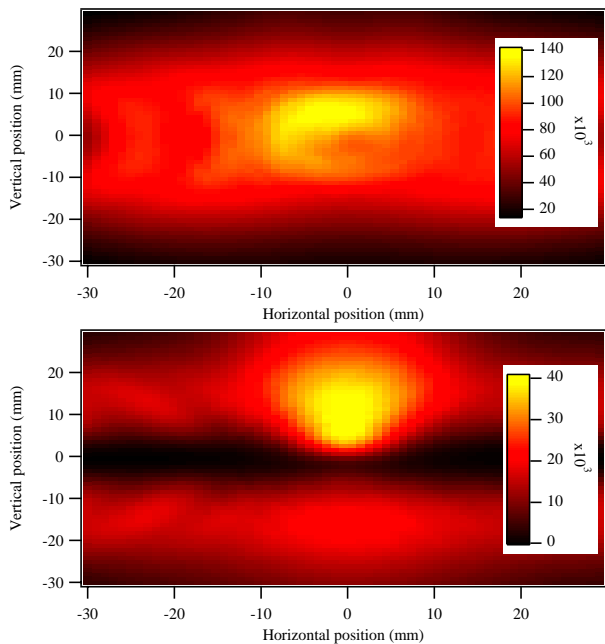


Figure 6: Transverse intensity distribution at 30 A excitation current, 10m behind the undulator centre, integrated from 300 nm to 3 μm (the range of Fig. 3). Horizontal polarization (top), vertical polarization (bottom). Units of the colour scale are photons/(nC mm²).

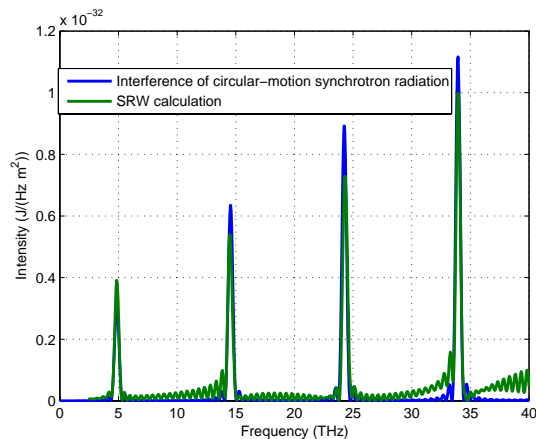


Figure 7: Comparison of the on-axis spectrum 9 m behind the undulator centre as calculated with SRW for the actual undulator field to the effect of interference of circular-motion synchrotron radiation from the individual undulator poles.

CONCLUSIONS

Exemplary calculations of the single-electron radiation generated by the FLASH infrared undulator are presented in this paper. Good agreement is found between different numerical codes. Such calculations allow incorporating a realistic source into Fourier optics codes to evaluate beam line performance and to interpret quantitatively spectral and intensity measurement results. The results presented suggest that angular filtering is needed to obtain well-defined resonance spectra.

REFERENCES

- [1] B. Faatz et al., Nucl. Instr. Meth. **A475**, 363 (2001)
- [2] G. Geloni et al., DESY 03-031 (March 2003)
- [3] O. Grimm, P. Schmüser, TESLA FEL 2006-03 (2006)
- [4] O. Grimm et al., Proc. of FEL 2005, Stanford, 21-26 August 2005, p. 183
- [5] V. Borisov et al., Proc. of EPAC 2006, Edinburgh, 26-30 June 2006, p.3596
- [6] N. Morozov et al., these proceedings
- [7] J.D. Jackson, *Classical Electrodynamics*, John Wiley & Sons, New York (1975)
- [8] G. Geloni et al., DESY 05-032 (February 2005)
- [9] O. Chubar, P. Elleaume, Proc. of the EPAC 1998, Stockholm, 22-26 June 1998, p.1177
<http://www.esrf.eu/Accelerators/Groups/InsertionDevices/Software/SRW>
- [10] <http://radiant.harima.riken.go.jp/spectra>
- [11] H. Wiedemann, *Particle Accelerator Physics II*, Springer, Berlin (1995)